Secoisolariciresinol dehydrogenase: mode of catalysis and stereospecificity of hydride transfer in *Podophyllum peltatum*

Syed G. A. Moinuddin,[a] Buhyun Youn,[c] Diana L. Bedgar,[a] Michael A. Costa,[a] Gregory L. Helms,[b] ChulHee Kang,[c] Laurence B. Davin[a] and Norman G. Lewis*[a]

Received 23rd November 2005, Accepted 4th January 2006
First published as an Advance Article on the web 30th January 2006
DOI: 10.1039/b516563f

Secoisolariciresinol dehydrogenase (SDH) catalyzes the NAD^+ dependent enantiospecific conversion of secoisolariciresinol into matairesinol. In *Podophyllum* species, (−)-matairesinol is metabolized into the antiviral compound, podophyllotoxin, which can be semi-synthetically converted into the anticancer agents, etoposide, teniposide and Etopophos®. Matairesinol is also a precursor of the cancer-preventative "mammalian" lignan, enterolactone, formed in the gut following ingestion of, for example, various high fiber dietary foods, as well as being an intermediate to numerous defense compounds in vascular plants. This study investigated the mode of enantiospecific *Podophyllum* SDH catalysis, the order of binding, and the stereospecificity of hydride abstraction/transfer from secoisolariciresinol to NAD^+. SDH contains a highly conserved catalytic triad (Ser^{153}, Tyr^{167} and Lys^{171}), whose activity was abolished with site-directed mutagenesis of Tyr167Ala and Lys171Ala, whereas mutagenesis of Ser153Ala only resulted in a much reduced catalytic activity. Isothermal titration calorimetry measurements indicated that NAD^+ binds first followed by the substrate, (−)-secoisolariciresinol. Additionally, for hydride transfer, the incoming hydride abstracted from the substrate takes up the *pro-S* position in the NADH formed. Taken together, a catalytic mechanism for the overall enantiospecific conversion of (−)-secoisolariciresinol into (−)-matairesinol is proposed.

Introduction

The lignans represent an abundant class of vascular plant natural products with important roles in human health protection,[1,2] pharmacology[3,4] and plant defense.[5–7] Elucidation of the biochemical pathways leading to their synthesis is resulting in systematic disentanglement of the lignin[8–10] and lignan[11–26] pathways which can overlap in the same tissue types, *e.g.* during heartwood formation. Of the various classes of lignans, entry into the pathway leading to many of the 8–8′-linked metabolites, such as matairesinol (**6**), podophyllotoxin (**7**) and plicatic acid (**8**), occurs *via* dirigent-mediated stereoselective coupling of *E*-coniferyl alcohol (**1**) to afford the furanofuran, (+)-pinoresinol (**2a**) (Fig. 1).[13,15,17,19,22,24] The latter can then undergo sequential NADPH-dependent reduction to afford (−)-secoisolariciresinol (**4a**) *via* catalysis by an enantiospecific pinoresinol-lariciresinol reductase.[11,12,14,20]

Of interest in this study is the next enantiospecific step converting (−)-secoisolariciresinol (**4a**) into (−)-matairesinol (**6a**) in the biochemical pathway to various lignans, such as to the antiviral/anticancer agent (−)-podophyllotoxin (**7**) in *Podophyllum* species.[17,18] Matairesinol (**6**) is also a precursor of the so-called "mammalian" lignan, enterolactone (**9**), which is believed to protect against onset of breast, prostate and colon cancers;[2,27,28] enterolactone (**9**) is formed in the gut by action of intestinal flora following ingestion of, for example, high fiber dietary foodstuffs.[29] Matairesinol (**6**) can also serve as an intermediate to various heartwood-protecting substances, such as plicatic acid (**8**) and its congeners, in western red cedar (*Thuja plicata*).[14,30–32]

In our earlier studies, secoisolariciresinol dehydrogenase (SDH†) was isolated from *Forsythia intermedia*, the encoding gene cloned (as well as one from *Podophyllum peltatum*), with the fully functional recombinant SDH so obtained characterized in terms of its basic kinetic parameters.[18] Additionally, we solved crystal structures of the apo-form and the corresponding binary/ternary complexes at 1.6 and 2.8/2.0 Å resolution, respectively.[25] *P. peltatum* SDH exists as a homotetramer in both solution and in the crystal lattice (D_2 symmetry), but whose ternary crystal complex (with NAD^+) could only be obtained with the product, (−)-matairesinol (**6a**), rather than the substrate, (−)-secoisolariciresinol (**4a**). Based on homology comparisons with other short-chain dehydrogenases,[25] it was provisionally concluded that SDH contained a conserved catalytic triad (Ser^{153}, Tyr^{167} and Lys^{171}).[33] In this study, we propose a mechanistic basis for this enantiospecific catalysis using both site-directed mutagenesis and isothermal calorimetery titration (ITC), with NMR spectroscopic analysis also being employed for determination of the stereospecificity of hydride transfer to NAD^+.

[a]*Institute of Biological Chemistry, Washington State University, Pullman, WA, 99164-6340, USA. E-mail: lewisn@wsu.edu; Fax: +1 509 335 8206; Tel: +1 509 335 2682*
[b]*NMR Center, School of Molecular Biosciences, Washington State University, Pullman, WA, 99164-4660, USA*
[c]*School of Molecular Biosciences, Washington State University, Pullman, WA, 99164-4660, USA*

† Abbreviations: Pp, *Podophyllum peltatum*; PLR, pinoresinol–lariciresinol reductase; SDH, secoisolariciresinol dehydrogenase; HMQC, heteronuclear multiple-quantum correlation.

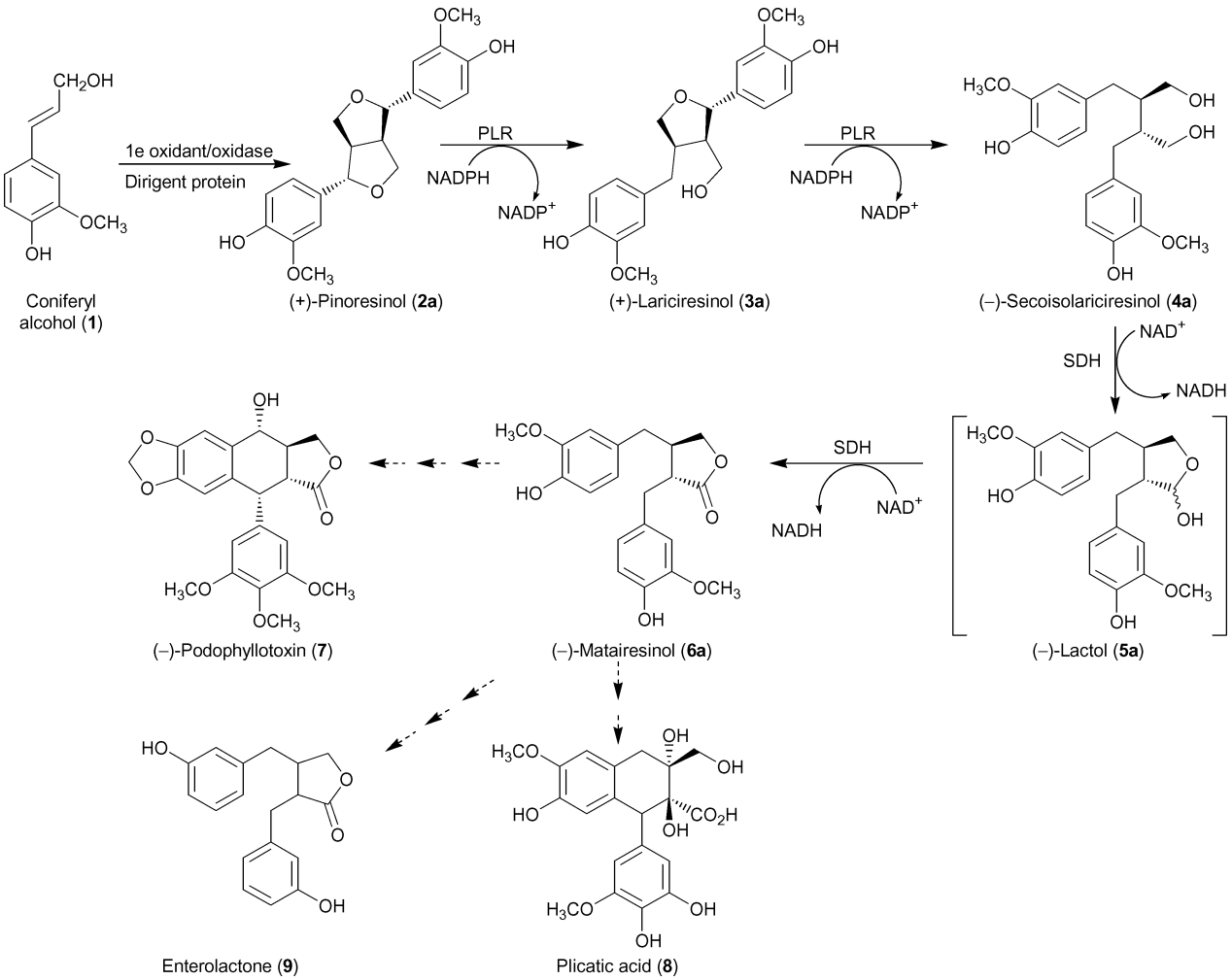

Fig. 1 Biochemical pathway to (−)-matairesinol (**6a**) in *F. intermedia* and *P. peltatum* and proposed conversions to (−)-podophyllotoxin (**7**) in *P. peltatum*, plicatic acid (**8**) in *T. plicata*, and to enterolactone (**9**) by action of intestinal flora. Opposite enantiomers (structures not shown) are depicted in the text as **2b** to **6b**.

Results and discussion

Site-directed mutagenesis of SDH catalytic triad

To determine the effect on the catalytic activity of SDH, site-directed mutagenesis of the proposed catalytic triad, Ser^{153}, Tyr^{167} and Lys^{171} of SDH_Pp7, was first carried out to individually mutate each of these residues into the hydrophobic non-reactive amino acid Ala. Mutations at each position [*i.e.* 153 (S → A), 167 (Y → A) and 171 (K → A)] (Table 1) were subsequently confirmed by sequencing each clone both in the forward and reverse directions (data not shown), as well as to ensure that no other point mutations were introduced during the PCR reactions. The three constructs were next individually transformed into *E. coli* TOP10 cells for protein expression and selected on carbenicillin, with the resulting clones designated as S153A, Y167A and K171A, respectively.

The mutagenized proteins (S153A, Y167A and K171A), as well as the wild type SDH_Pp7, were then first individually purified (*circa* 97% purity by silver staining) by anion exchange chromatography and assayed for their capacity to convert secoisolariciresinol (**4**) into either the intermediary lactol (**5**) or matairesinol (**6**). SDH_Pp7 and the mutants, S153A, Y167A and K171A, were thus individually incubated with (±)-secoisolariciresinols (**4a/b**) in the presence of NAD^+ and the products separated by HPLC as described in the Experimental section. As indicated in Table 2, enzymatic activity was abolished when SDH was mutated at either position Tyr^{167} or Lys^{171}. The S153A mutant, by contrast, displayed

Table 1 Primers used for site-directed mutagenesis of SDH amino acid residues Ser^{153}, Tyr^{167} and Lys^{171} to Ala

Mutation	5′ Primer	3′ Primer
S153 → A153	5′ GTATTCACTGCA**GCT**ATTTCTTCCTTCACAGC 3′	5′ GCTGTGAAGGAAGAAAT**AGC**TGCAGTGAATAC 3′
Y167 → A167	5′ GGTGTGTCGCATGTT**GCC**ACCGCAACCAAG 3′	5′ CTTGGTTGCGGT**GGC**AACATGCGACACACC 3′
K171 → A171	5′ GTTTACACCGCAACC**GCG**CATGCTGTCCTTGG 3′	5′ CCAAGGACAGCATG**CGC**GGTTGCGGTGTAAAC 3′

Table 2 Conversion of (−)-secoisolariciresinol (**4a**) by wild type secoisolariciresinol dehydrogenase and three mutants (S153A, Y167A and K171A)[a]

Protein	(−)-Lactol (**5a**) pmol min^{-1} μg^{-1} prot	(−)-Matairesinol (**6a**) pmol min^{-1} μg^{-1} prot
Wild type	nd[b]	3.5 ± 0.02
S153A	0.2 ± 0.01	nd
Y167A	nd	nd
K171A	nd	nd

[a] the (+)-antipode (**4b**) did not serve as substrate, [b] nd, not detected.

very modest activity as evidenced by a relatively poor conversion of (−)-secoisolariciresinol (**4a**) into (−)-lactol (**5a**); however, no further conversion of **5a** into (−)-matairesinol (**6a**) was observed. Moreover, there was no further restoration of activity when the mutated proteins were purified to apparent homogeneity (data not shown). These data were, therefore, consistent with the proposed involvement of the catalytic triad for conversion of (−)-secoisolariciresinol (**4a**) into (−)-matairesinol (**6a**).

The mode of SDH-catalyzed hydride transfer to NAD^+ from either substrate (−)-secoisolariciresinol (**4a**) or the intermediary (−)-lactol (**5a**) was next investigated, and whether this involved stereospecific hydride transfer to either the *pro-R* or *pro-S* (hydrogens) at C-4 of the NADH so formed.

Synthesis of [4*R*–^{2}H] and [4*S*–^{2}H]NADH

To experimentally differentiate between the above possibilities, [4*R*–^{2}H] and [4*S*–^{2}H]NADH were first enzymatically synthesized.[34] The [4*R*–^{2}H]-nicotinamide adenine dinucleotide (NADD) was prepared by incubating NAD^+ in the presence of ethanol-d_6, horse liver alcohol dehydrogenase and yeast aldehyde dehydrogenase, whereas [4*S*–^{2}H]NADH was prepared by incubating NAD^+ with D-glucose-1-*d* and *Leuconostoc mesenteroides* glucose-6-phosphate dehydrogenase[34] (see Experimental section). The reduced nucleotides so formed were then individually purified *via* a combination of DEAE cellulose and Bio-Gel P-2 column chromatographic steps, with fractions of interest containing NADD (A_{260} : A_{340} ratio <2.3) individually pooled and lyophilized.

The stereochemistry and isotopic purity of the two distinct forms of deuterated NADD [4*R*- and 4*S*–^{2}H] were individually established by analysis of the ^{1}H and heteronuclear multiple-quantum correlation (HMQC) spectra, together with comparison to undeuterated (natural abundance) NADH.[35–38] In the ^{1}H NMR spectrum of unlabelled NADH (Sigma, 98% pure and containing 0.47% EtOH) in D_2O (Fig. 2A and inset), the two C-4 protons in the dihydropyridine ring were clearly observed with resonances for the 4*S*-proton centered at δ 2.65 ppm (m, J_{4S-4} 18.3, J_{4S-5} 3.5, J_{4S-6} 0.8, J_{4S-2} 1.0 Hz) and for the 4*R*-proton centered at δ 2.77 ppm (m, J_{4R-4} 18.3, J_{4R-5} 2.8, J_{4R-6} 2.2, J_{4R-2} 0.8 Hz). By contrast, examination of the enzymatically generated forms of NADD established that both were ~91% deuterated at the C-4 position as determined by integration of the 1D ^{1}H NMR spectrum. Furthermore, the 4*R* proton of [4*S*–^{2}H]NADH (Fig. 2B and inset) gave a broad signal at δ 2.75 ppm (J_{4R-5} 2.7 Hz), indicating loss of the 18.3 Hz geminal coupling thereby establishing that the deuterium atom resides at the 4*S* position, whereas the 4*S* proton of [4*R*–^{2}H]NADH (Fig. 3C and inset) appeared as a broad doublet (J_{4S-5} 3.5 Hz) at δ 2.63 ppm, again displaying loss of the 18.3 Hz geminal coupling. The resonances also showed upfield shifts of

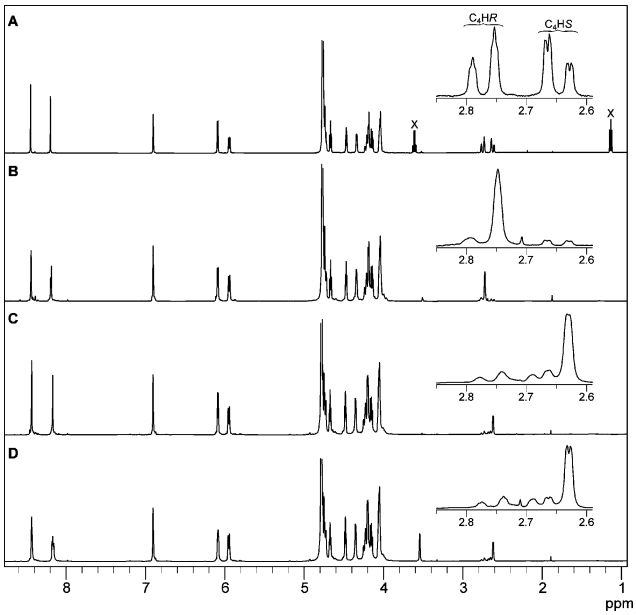

Fig. 2 ^{1}H NMR spectra of NADH with inset showing spectroscopic regions for 4*S* and 4*R* protons at C-4 of the dihydropyridine ring. (A) Natural abundance NADH (Sigma, 0.47% EtOH). (B) [4*S*–^{2}H]NADH. (C) [4*R*–^{2}H]NADH. (D) Enzymatically synthesized [4*R*–^{2}H]NADH with SDH_Pp7 following incubation with (±)-secoisolariciresinols (**4a/b**) and [4-^{2}H]NAD^+. X = Solvent (EtOH).

~18–20 ppb due to the geminal deuterium isotope effect.[39] The data so obtained were thus in good agreement with that of Arnold *et al.*,[36] Velonia *et al.*[37] and Mostad and Glasfeld.[38]

In the unlabelled NADH sample, the HMQC experiment shows two sets of cross-peaks centered at 24.40 ppm in F1 which belong to the diastereotopic protons that reflect the large geminal coupling between the 4*R* and 4*S* protons. The 4*S* set is centered at 2.65 ppm in F2, with the doublet signals appearing at 2.62 and 2.67 ppm while the 4*R* set is centered at 2.77 ppm in F2 with the doublet components appearing at 2.75 and 2.80 ppm in the 2D contour plot (see Fig. 3A). By contrast, HMQC analysis of [4*S*–^{2}H]NADH revealed loss of the *pro-R* proton cross-peak at δ 2.62, F2 (^{1}H) (Fig. 3B) thereby establishing the deuterium atom to be at the 4*S* position. In an analogous manner, analysis of the [4*R*–^{2}H]NADH (Fig. 3C) established absence of the *pro-S* cross-peak at δ 2.75, F2 (^{1}H) thereby placing the deuterium atom at 4*R*.

Synthesis of [4-^{2}H]NAD^+

With the two distinct forms of NADD (4*R*- and 4*S*–^{2}H) unambiguously distinguished, the stereospecificity of hydride transfer from the substrates (−)-secoisolariciresinol (**4a**)/(−)-lactol (**5a**) to

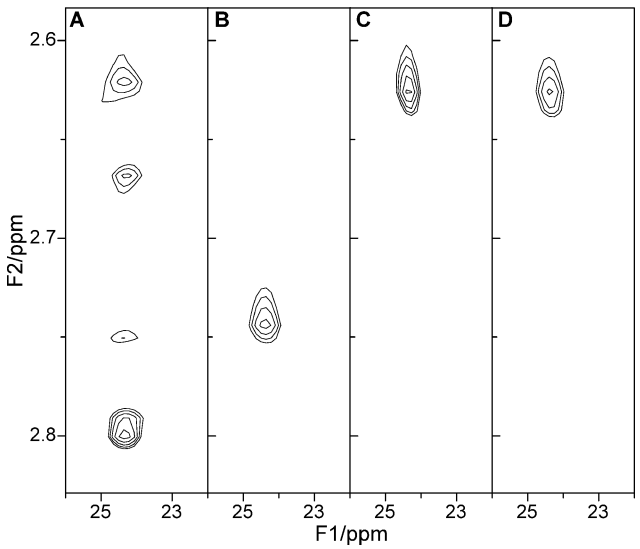

Fig. 3 Expanded regions of the HMQC spectra of NADH (C-4 hydrogens and C-4 carbon). (A) Natural abundance NADH. (B) [4*S*–^{2}H]NADH. (C) [4*R*–^{2}H]NADH. (D) Enzymatically synthesized [4*R*–^{2}H]NADH following incubation with (±)-secoisolariciresinols (**4a/b**) and [4-^{2}H]NAD$^+$ with SDH_Pp7.

NAD$^+$ during SDH catalysis was investigated using [4-^{2}H]NAD$^+$ as cofactor. The latter was obtained by oxidizing [4*R*–^{2}H]NADH with rabbit muscle *α*-glycerophosphate dehydrogenase in the presence of dihydroxyacetone phosphate,[40] with the enzymatically formed [4-^{2}H]NAD$^+$ purified further by gel permeation chromatography on Bio-Gel P-2 (see Experimental section).

Comparison of the ^{1}H NMR-spectra of the resulting [4-^{2}H]NAD$^+$ (Fig. 4B) with that of unlabelled NAD$^+$ (Fig. 4A), was carried out in a manner analogous to that for NADH. The unlabelled NAD$^+$ displayed a signal at δ 8.81 ppm (brdt, J_{4H-5H} 8.0, J_{4H-6H} 1.2, J_{4H-2H} 1.2 Hz) for the pyridinium proton at C-4 (Fig. 4A). By contrast, analysis of the ^{1}H NMR spectrum of the [4-^{2}H]NAD$^+$ (Fig. 4B) revealed that the resonance at δ 8.81 was ~88% diminished, relative to unlabelled NAD$^+$ (based on ^{1}H NMR integration) in accordance with C-4 being specifically deuterated. This was further confirmed by the change in the multiplicity at δ 8.17 of the C-5 proton, *i.e.* from a dd (J_{5H-4H} 8.0, J_{5H-6H} 6.3 Hz, Fig. 4A) to a doublet (J_{5H-6H} 6.3 Hz, Fig. 4B).

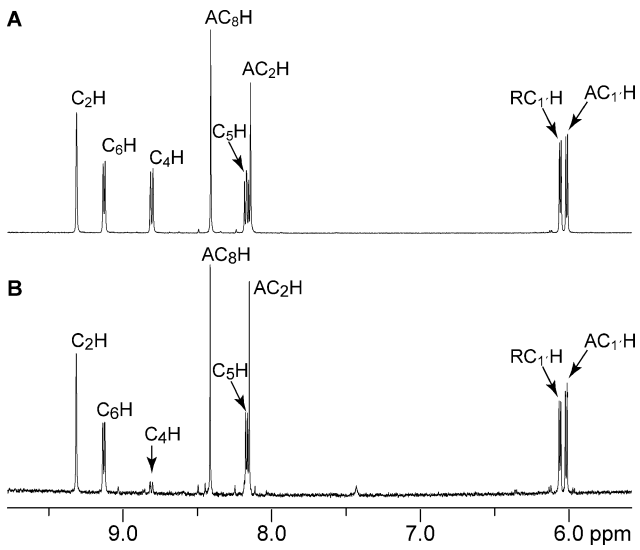

Fig. 4 Expansion of aromatic region of the ^{1}H NMR spectra of NAD$^+$. (A) Natural abundance NAD$^+$ (Sigma). (B) [4-^{2}H]NAD$^+$. Resonances denoted by C_2H, C_4H, C_5H and C_6H are from protons at carbons 2, 4, 5 and 6 of the pyridine ring, respectively, whereas AC_2H and AC_8H are those at carbons 2 and 8 of the adenine (A) ring. $RC_{1'}H$ and $AC_{1'}H$ refer to the anomeric carbons of the ribose rings in NAD$^+$, respectively.

Generation of NADD during SDH catalysis

(±)-Secoisolariciresinols (**4a/b**) were thus next incubated with a partially purified SDH preparation (see Experimental section) in the presence of [4-^{2}H]NAD$^+$. LC–APCI–MS analysis of the resulting enzymatically generated matairesinol (**6**) (retention time 16.02 min) then gave a molecular ion [M$^+$] at *m/z* 358.16 confirming its identity. Its optical purity was also established using the procedure of Xia *et al.*,[18] thus confirming that only the (−)-antipode (**6a**) was formed (data not shown).

The aqueous phase containing the SDH generated NADH was next purified as previously described above for [4*R*–^{2}H] and [4*S*–^{2}H]NADH. The ^{1}H NMR and HMQC analyses of the resulting NADH generated during SDH catalysis revealed the presence of a broad doublet at δ 2.63 ppm (J_{4S-5} 3.0 Hz) again showing loss of the 18.3 Hz geminal coupling, and absence of the *pro-S* crosspeak at δ 2.77 (Figs. 2D and 3D), *i.e.*, establishing that the deuterium in the enzymatically generated NADD was at the 4*R* position. Thus, the hydride abstracted from either (−)-secoisolariciresinol (**4a**) or the (−)-lactol (**5a**) to [4-^{2}H]NAD$^+$ occurred in such a manner whereby hydride addition is at the B-face of the nicotinamide ring of NAD$^+$ giving [4*R*–^{2}H]NADD, and thus establishing SDH to be a B-type dehydrogenase. These data confirm the prediction made from the previous X-ray crystallographic analysis,[25] which suggested [from analysis of the ternary complex with (−)-matairesinol (**6a**) rather than (−)-secoisolariciresinol (**4a**)] that the B-face of the nicotinamide ring was open to the cleft with the C-4 of the nicotinamide ring being ~5 Å from the target hydroxyl group of the substrate **4a**. The current study now demonstrates that both the nicotinamide and the substrate are in the proper orientation for B-face specific hydride transfer to C-4 from the substrates [(−)-secoisolariciresinol (**4a**)/lactol (**5a**)].

Isothermal titration calorimetry

Isothermal titration calorimetry (ITC)[41–43] was next employed to study SDH_Pp7 in terms of its NAD$^+$ cofactor-binding characteristics and differential ligand affinity between the enantiomeric substrates **4a** and **4b**. In every case, the calorimetric data revealed that heat was released when enantiomerically pure substrates **4a** and **4b** and cofactor were individually associated with SDH_Pp7, indicating that those interactions had significant enthalpic contributions in binding (Table 3). It also revealed slightly unfavorable entropic contributions for each, possibly indicating that the enzyme was slightly stabilized upon binding. This effect is especially noticeable for NAD$^+$, as previously indicated by the significant reduction of B-values of one loop constituting the binding pocket upon formation of the NAD$^+$ binary complex.[25] As shown in Fig. 5 and Table 3, both (−)- and (+)-secoisolariciresinols **4a** and **4b** showed comparable binding

Table 3 SDH_Pp7 binding parameters determined by isothermal titration calorimetry

Compound(s)	K_d/μM	ΔH/kcal mol^{-1}	ΔS/cal mol^{-1} degree^{-1})
4a	44.5 ± 3.4	−19.4 ± 0.8	−45.1
4b	50.6 ± 3.7	−22.9 ± 1.0	−57.0
NAD$^+$	5.5 ± 0.3	−28.6 ± 0.8	−76.5
NAD$^+$/**4a**	2.3 ± 0.1	−12.2 ± 0.1	−15.2
NAD$^+$/**4b**	4.5 ± 0.7	−25.7 ± 0.7	−43.3

affinities to SDH_Pp7 in the absence of NAD$^+$. However, when the latter is present, there is a 10–20 fold decrease in K_d values, with a significant difference (~2 fold) in binding of the (−)-antipode **4a** ($K_d = 2.3$ μM) over that of the (+)-enantiomer **4b** ($K_d = 4.5$ μM). This is indicative of a significant involvement of NAD$^+$ to facilitate binding interactions of the substrate, even though only **4a** is processed catalytically. Taken together, we interpret the ITC data as indicating that NAD$^+$ binds first, followed by the substrate, with catalytic conversion of (−)-**4a**, and NADH leaving last.

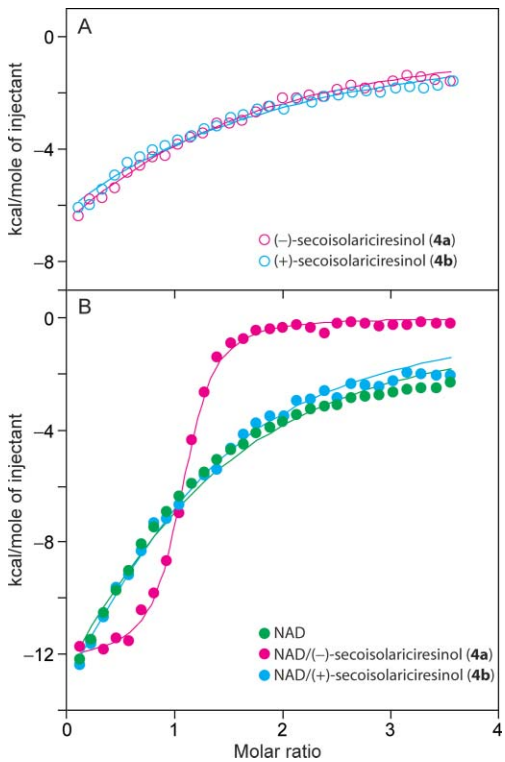

Fig. 5 Heat of injection experimentally determined during titration of potential substrates and cofactor in the presence of SDH_Pp7. (A) With (−)- and (+)-secoisolariciresinols (**4a** and **4b**). (B) With NAD$^+$ alone, together with (−)- and (+)-secoisolariciresinols (**4a** and **4b**). Solid lines represent the least square fits of the data using a one-site binding model.

Catalytic mechanism of SDH

Based on the predictions from X-ray crystal structural analysis,[25] and the results from the current study, a catalytic mechanism for SDH can now be proposed (Fig. 6). Beginning with the apo-SDH_Pp7 structure (Fig. 6A), several water molecules form a hydrogen bonded network with the hydroxyl, quaternary ammonium and phenolic groups of the highly conserved catalytic triad residues, *i.e.* of Ser^{153}, Lys^{171} and Tyr^{167}. Binding of NAD$^+$ (shown as [4-^{2}H]NAD$^+$) then releases the bound water molecules in an entropically favorable manner, with the phenolic and quaternary ammonium groups at Tyr^{167} and Lys^{171} hydrogen bonded to the 2′ and 3′ hydroxyl groups of the ribosyl ring, respectively, thereby fixing the position of the cofactor during catalysis (Fig. 6B). Binding of NAD$^+$ to Lys^{171} in this way favors deprotonation of the phenolic Tyr^{167} group, thus lowering its pK_a, with the resulting phenolate anion being further stabilized by hydrogen bonding to the Ser^{153} hydroxyl group. Following substrate binding, the Tyr^{167} phenolate group then serves as a general base in substrate deprotonation and hence facilitates hydride transfer during SDH catalysis as demonstrated in this study.[25]

Deprotonation of the bound (−)-secoisolariciresinol (**4a**) is next followed by concomitant intramolecular cyclization/hydride transfer (Fig. 6C), to afford the intermediary lactol (−)-**5a**, *i.e.* where hydride addition occurs at the B face of [4-^{2}H]NAD$^+$ to produce [4*R*–^{2}H]NADH (Fig. 6D). The latter is then released from the active site since the Tyr^{167} phenolic group no longer holds the resulting neutral NADH. In an analogous manner, the subsequent conversion of (−)-lactol (**5a**) to (−)-matairesinol (**6a**) involves binding of a second molecule of [4-^{2}H]NAD$^+$ as before, with reiteration of the catalytic process (Figs. 6E and 6F), thereby generating a second molecule of [4*R*–^{2}H]NADH and the final product, (−)-matairesinol (**6a**). Thus, the overall SDH-mechanism envisaged is concerted.

Conclusion

SDH belongs to the large, functionally heterogeneous, SDR protein family, with the latter being of increasing scientific interest since several are correlated with hormone-dependent cancers, obesity, diabetes, and infectious diseases.[44] In our studies, analysis of SDH X-ray crystal structure, site-directed mutagenesis and NMR spectroscopic data have resulted in delineation of the catalytic mechanism including that of the role of the conserved residues. Site-directed mutagenesis of two of the catalytic triad residues (Tyr^{167} and Lys^{171}) completely abolished catalytic activity, this being presumably explicable on the basis of their direct roles in catalysis and in binding of the ribose unit within NAD$^+$ by Tyr^{167}/Lys^{171}. While replacement of Ser^{153} by Ala^{153} did not result in complete abolition of SDH activity, it nevertheless plays an important role in catalysis since only modest amounts of lactol (**5a**) were formed but not (−)-matairesinol (**6a**) with the S153A mutant. Lastly, our cumulative sequence data, detailed 3-D structures and knowledge of the catalytic mechanism of the participating enzymes in the lignan biosynthetic pathway are systematically providing a comprehensive understanding of their physiological roles in vascular plants. This will also facilitate the opportunity to initiate metabolic engineering approaches that should provide a facile source of these beneficial lignans in foodstuffs or of antiviral/anticancer lignans, such as podophyllotoxin.

Experimental

Materials

Horse liver alcohol dehydrogenase, yeast aldehyde dehydrogenase, *Leuconostoc mesenteroides* glucose-6-phosphate dehydrogenase

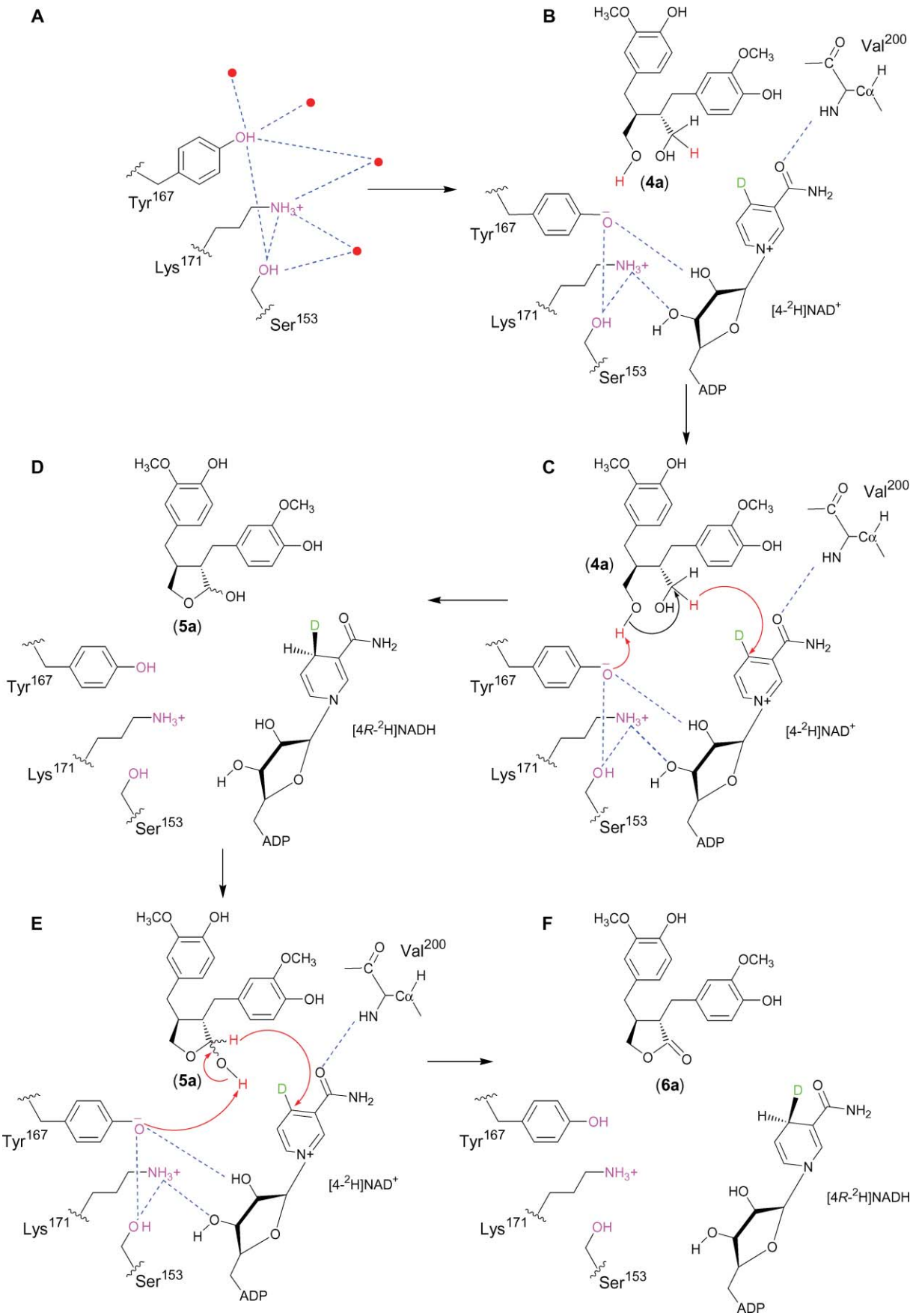

Fig. 6 Proposed catalytic mechanism of SDH_Pp7.

and rabbit muscle α-glycerophosphate dehydrogenase were purchased from Sigma-Aldrich, as well as ethanol-d_6 (99.5 atom %D), D-glucose-1-*d* (97 atom %D), β-NAD^+ (sodium salt), NADH (98% pure, disodium salt), DEAE cellulose and dihydroxyacetone phosphate (dilithium salt). D_2O (99.96 atom% D) was obtained from Cambridge Isotope Lab, Inc., MA, whereas Bio-Gel P-2 (45–90 μm) was purchased from Bio-Rad Laboratories. All other solvents and chemicals used were reagent or HPLC grade.

Analytical methods

UV spectra were recorded on a Perkin-Elmer Lambda 20 UV–VIS instrument. HPLC analyses were carried out using an Alliance 2695 HPLC system (Waters, Milford, MA) with detection at 280 nm. Reversed-phase HPLC used a NovaPak C_{18} column (150 × 3.9 mm, Waters) with the following elution conditions at a flow rate of 1 cm^3 min^{-1}: linear gradients of CH_3CN: 3% (v/v) AcOH in H_2O from 10 : 90 to 35 : 65 between 0 and 15 min, then to 95 : 5 in 5 min with this composition held for an additional 2 min, and finally returned back to 10 : 90 in 2 min, this being held for 15 min. Chiral HPLC separations of (+)- and (−)-secoisolariciresinols (**4a**) and (**4b**) employed a Chiralcel OD (Chiral Technologies, Inc.) column (250 × 4.6 mm) eluted with hexanes : EtOH (7 : 3) at a flow rate of 0.5 cm^3 min^{-1}.[17,45] Liquid chromatography-mass spectrometry with an atmospheric pressure chemical ionization interface system (LC–APCI–MS) was performed using a Finnigan MAT (San Jose, CA, USA) ion trap mass spectrometer equipped with a Finnigan electrospray interface, with LC separations being carried out on an Alliance Instrument as described above for HPLC analyses. A fast-protein liquid chromatography (FPLC, Amersham Pharmacia Biotech) and a BioCad (Applied Biosystems) systems were used for purification of reduced nucleotides and SDH, respectively.

NMR spectroscopy

One dimensional ^1H and two dimensional HMQC spectra were collected on a Varian Inova 500 MHz spectrometer operating at 499.85 MHz for ^1H and 125.67 MHz for ^{13}C, respectively. Proton spectra obtained in D_2O were referenced to the TSP (sodium-3-trimethylsilyl-(2,2,3,3-d_4)propionate) proton signal at 0.0 ppm, whereas the ^{13}C dimension of the HMQC spectra was referenced indirectly to the TSP signal *via* the method described by Wishart *et al.*[46] *J* values for the dihydropyridine ring of NADH were calculated by extensive homonuclear spin decoupling and simulation using the MestRe-C program.[47] Gradient enhanced phase-sensitive HMQC spectra were obtained using the standard Varian pulse sequence, with HMQC spectra collected with sweep widths (acquisition times) of 4,668 Hz (219 ms) in t2 (^1H) and 18854 Hz (6.8 ms, 128 × 2 hypercomplex increments or 27.2 ms for 512 × 2 hypercomplex increments) in t1 (^{13}C). Data were processed in F2 by applying a Gaussian function with a 0.101 s time constant prior to Fourier transformation. The F1 processed data utilized a linear prediction of the original 128 real points, in the case of data sets acquired for 6.8 ms in t1, to 256 points, apodizing with a Gaussian function with a 0.011 s time constant followed by zero filling to 2 K complex points, followed by Fourier transformation leading to digital resolution of 4.6 Hz pt^{-1} in F2 and 18.4 Hz pt^{-1} in F1. Data sets collected for 27.2 ms in t1 were first extended by linear prediction from 512 real points to 1024 real points followed by apodization with a Gaussian function of 0.033 s time constant, zero filled to 4 K complex points and Fourier transformed to give digital resolution of 4.6 Hz pt^{-1} in F2 and 9.2 Hz pt^{-1} in F1.

Synthesis of (−)-and (+)-secoisolariciresinols 4a and 4b

Racemic (±)-pinoresinols (**2a**/**2b**) were synthesized as described in Xia et al.[18] by oxidative coupling of *E*-coniferyl alcohol (**1**) with $FeCl_3$. The racemate **2a**/**2b** was then resolved using a Chiralcel OD (Chiral Technologies, Inc.) column[48] to give the (+)-(**2a**, 21.1 mg) and (−)-(**2b** 24.0 mg) antipodes, respectively. Enantiomerically pure (+)- and (−)-pinoresinols (**2a** and **2b**) were next individually converted to (+)-(**3a**, 7.8 mg) and (−)-(**3b**, 8.8 mg) lariciresinols together with (−)-(**4a**, 3.0 mg) and (+)-(**4b**, 4.0 mg) secoisolariciresinols, respectively, as described in Katayama *et al.*[49]

Synthesis of deuterated NADH and NAD^+

[4*R*–^{2}H]NADH. The synthesis and purification of [4*R*–^{2}H]NADH was carried out as described by Viola *et al.*[34] and Anderson and Lin,[50] respectively, with the following modifications: Ethanol-d_6 (2.8 mM) was incubated with NAD^+ (5.6 mM), horse liver alcohol dehydrogenase (50 units), and yeast aldehyde dehydrogenase (100 units), with the reaction monitored by following the increase in absorbance at 340 nm. After completion of the reaction (3 h), carbon tetrachloride (1 cm^3) was added to the reaction mixture, with the whole vortexed and centrifuged (290g, 5 min). The aqueous phase (∼10 cm^3) containing the reduced nucleotide was next filtered (0.45 μm) and applied to a DEAE cellulose column (1.6 × 40 cm) previously equilibrated in 10 mM Tris-base buffer (pH 9.2). After washing the column with the same buffer (35 cm^3), [4*R*–^{2}H]NADH was next eluted (and separated from unreacted NAD^+) with a linear gradient of NaCl (from 0 to 0.4 M) in 10 mM Tris-base buffer (pH 9.2) over 150 min, at a flow rate of 1 cm^3 min^{-1} and with detection at 280 nm. Fractions containing [4*R*–^{2}H]NADH and having a A_{260} : A_{340} ratio of less than 2.4 were individually pooled, desalted on a Bio-Gel P-2 column (2.6 × 40 cm) equilibrated in distilled H_2O (pH 9.0) at a flow rate of 0.8 cm^3 min^{-1}, then combined, lyophilized and stored at −80 °C. The isotopic purity of [4*R*–^{2}H]NADH was determined by ^1H NMR and HMQC spectroscopic analyses to be ∼89%.

[4*S*–^{2}H]NADH. The synthesis of [4*S*–^{2}H]NADH was carried out as described by Viola *et al.*[34] by incubating D-glucose-1-*d* (13.5 mM, 10 mg), NAD^+ (12.1 mM, 34 mg) and *Leuconostoc mesenteroides* glucose-6-phosphate dehydrogenase (42 units), but with the following modifications: the reaction progress was monitored by measuring the increase in absorbance at 340 nm and was completed by 28 h, at which point the 260 to 340 nm ratio was 2.3. Carbon tetrachloride (1 cm^3) was then added to the reaction mixture, with the whole vortexed and centrifuged (290g, 5 min). After reduction of the aqueous phase volume to two thirds of its original volume under reduced pressure at 35 °C, [4*S*–^{2}H]NADH was purified as described above for [4*R*–^{2}H]NADH. The isotopic purity was again determined by ^1H NMR and HMQC spectroscopic analyses to be ∼91%.

[4-^{2}H]NAD^+. This was enzymatically synthesized as described by Oppenheimer[40] by incubating [4*R*–^{2}H]NADH (5 mg, 0.48 mM),

dihydroxyacetone phosphate (25.5 mg; 9.3 mM) and rabbit muscle α-glycerophosphate dehydrogenase (460 units) at 30 °C for 8 to 10 h, at which time solid trichloroacetic acid was added. After centrifugation (290g, 10 min), the supernatant was lyophilized, with the resulting residue reconstituted in H_2O (1 cm^3).[40] This solution was next applied to a Bio-Gel P-2 column (1.6 × 100 cm) equilibrated in distilled water (pH 7.5) at a flow rate of 0.3 cm^3 min^{-1} in order to separate [4-^{2}H]NAD^+ from unreacted [4*R*–^{2}H]NADH. Fractions that absorbed at 260 nm were pooled and lyophilized. The isotopic purity of [4-^{2}H]NAD^+ was determined by ^{1}H NMR spectroscopic analysis to be ~88%.

Expression and partial purification of SDH

Podophyllum peltatum SDH_Pp7, cloned into an Invitrogen pTrcHis2-TOPO® TA vector, was transformed and expressed into TOP10 *E. coli* as previously described.[18] The cell pellet containing SDH_Pp7 was suspended in BugBuster (10 cm^3), lysozyme (10 kilounits mm^{-3}, 1 mm^3) and benzonase (25 units mm^{-3}, 10 mm^3). After shaking at room temperature for 10 min, the slurry was centrifuged (8,000g, 10 min). The supernatant was next subjected to $(NH_4)_2SO_4$ precipitation, with the proteins precipitating between 20 to 60% $(NH_4)_2SO_4$ reconstituted in buffer A (50 mM Tris-HCl, pH 7.5), and further desalted over PD-10 columns (Amersham Pharmacia Biotech). The desalted fraction was then applied to a DEAE cellulose column (2.5 × 27 cm) equilibrated with buffer A at a flow rate of 1 cm^3 min^{-1}. After washing the column with buffer A (5 cm^3), SDH_Pp7 was eluted as follows: linear NaCl gradients in buffer A first from 0 to 1 M in 100 cm^3 and then from 1 to 2 M in 20 cm^3 with this final NaCl concentration held for another 10 cm^3. The SDH_Pp7 containing fractions, eluted at ~0.2 M NaCl were combined, concentrated and desalted into Buffer A by ultrafiltration (Amicon cell) using a 10 kDa cut-off membrane (Millipore). The concentrated SDH_Pp7 was next applied to a POROS HQ anion exchange (4.6 × 100 mm) column equilibrated in buffer A at a flow rate of 7 cm^3 min^{-1}. After washing the column with buffer A (3.3 cm^3), proteins were next eluted with NaCl linear gradients first from 0 to 0.3 M in buffer A (50 cm^3) and then to 1 M (8.3 cm^3), with this final concentration further held for 3.3 cm^3. Fractions containing SDH_Pp7 eluting between 0.13 and 0.17 M NaCl were combined, desalted and subjected to POROS HQ chromatography under the same conditions as above, with fractions containing SDH_Pp7 combined and directly used for assays.

Site-directed mutagenesis of SDH_Pp7

Primers (Table 1) were designed and synthesized (Invitrogen, Carlsbad, USA) to individually convert Ser^{153}, Tyr^{167} and Lys^{171} in *Podophyllum peltatum* SDH_Pp7 into the hydrophobic non-reactive alanine. Site specific mutations were performed using a QuikChange XL site-directed mutagenesis kit (Stratagene, La Jolla, USA) following the manufacturer's instructions with PCR conditions modified as follows: initial denaturation at 95 °C for 1 min, 18 cycles at 95 °C for 1 min, 60 °C for 1 min and 68 °C for 7 min, followed by *Dpn* I digestion and transformation into XL10 Gold® ultracompetent *E. coli* cells. Transformants were selected on LB plates containing 100 μg cm^{-3} carbenicillin. Positive clones containing a single point mutation at positions 153 (S → A), 167 (Y → A) and 171 (K → A), respectively, were confirmed by sequencing using pTrcHis2 forward and reverse primers (Invitrogen) flanking the gene. Both strands were completely sequenced using an automated DNA sequencer with Big-Dye™ terminator technology to ensure that there were no other mutation(s) in the open reading frame as a result of PCR. The three constructs were individually transformed into the *E. coli* strain TOP 10 (Invitrogen) for protein expression, and selected on LB plates containing 100 μg cm^{-3} carbenicillin. The resulting clones were designated as S153A, Y167A and K171A, respectively. Individual mutant lines (S153A, Y167A and K171A) were next grown overnight in LB medium, with the heterologously expressed proteins purified and assayed for (−)-matairesinol (**6a**) formation as described above for wild type SDH_Pp7.

SDH assays

Matairesinol (6) formation. Each assay consisted of (±)-secoisolariciresinols (**4a/b**, 5 mM, 10 mm^3), NAD^+ (10 mM, 10 mm^3), the purified SDH_Pp7 or mutant, S153A, Y167A and K171A (1 to 4 μg) and Tris-HCl buffer (50 mM, pH 8.8) to a final volume of 200 mm^3. After incubation for 10 min at room temperature, the reaction was stopped by addition of glacial AcOH (10 mm^3). An aliquot (80 mm^3) was next subjected to reversed-phase HPLC to separate **4** from the products **5** and **6** (see Analytical methods section).

[4-^{2}H]NADH formation. To assay mixtures consisting of (±)-secoisolariciresinols (**4a/b**) (5 mM in MeOH, 0.61 cm^3), 50 mM Tris-HCl buffer (pH 8.8, 9.29 cm^3) and [4-^{2}H]NAD^+ [4.2 mg in 50 mM Tris-HCl buffer (pH 8.8), 2 cm^3] was added the partially purified SDH_Pp7 as described above (0.305 cm^3, 884.5 μg). After incubation at room temperature with shaking for 10 min, the reaction mixture was quenched with EtOAc (6 cm^3). To establish the integrity of the enzymatic reaction, the EtOAc solubles were dried (Na_2SO_4) and evaporated to dryness *in vacuo*. The EtOAc-derived residue was reconstituted in MeOH (2 cm^3) with an aliquot (20 mm^3) subjected to reversed-phase HPLC analysis with the enzymatically formed matairesinol (**6a**) identified by LC–APCI–MS analysis as described in the Analytical methods section. The chirality of the enzymatically formed matairesinol (**6**) was determined as previously described.[17,45] Finally, the aqueous phase was subjected to centrifugation (1,200g, 10 min), filtered (0.45 μm), with the enzymatically formed [4-^{2}H]NADH purified as described above. Fractions containing [4-^{2}H]NADH were pooled, lyophilized and subjected to ^{1}H NMR and HMQC spectroscopic analyses.

Isothermal titration calorimetry (ITC)

Isothermal titration calorimetry (ITC)[41–43] was performed at 25 °C using a VP-ITC instrument (MicroCal, Northampton, MA). Enantiomerically pure substrates **4a** and **4b** were first individually dissolved in MeOH (0.3 cm^3, 48 mM), with buffer B (20 mM Tris, pH 8.0, 1 mM DTT, 1 mM EDTA, 10% glycerol) next added such as the MeOH content was 1% and the final concentration of either **4a** or **4b** was 0.48 mM. NAD^+ (0.48 mM) was dissolved in buffer A containing 1% MeOH. Purified SDH_Pp7[25] was dialyzed extensively against buffer B in an Amicon stirred cell at 4 °C, after which MeOH was added to give a 1% final concentration. The

final enzyme concentration (30 μM of monomer) was determined by the Bradford method[51] using BSA as standard. Both the enzyme and substrate/cofactor solutions were individually degassed *in vacuo* for 5 min before ITC. Titration experiments were performed as follows: aliquots (10 mm^3) of the ligand solution (**4a**, **4b** or NAD) were injected into the reaction cell containing SDH_Pp7 (2 cm^3) with stirring set at 300 rpm. Twenty nine injections for each assay condition were performed with an equilibration interval of 400 s between each.

Binary complex titrations were individually carried out by adding **4a**, **4b** or NAD^+ solution to the SDH_Pp7 solution in the reaction cell. Ternary complex titrations were carried out by mixing SDH_Pp7 and NAD^+ in a 1 : 1 ratio (30 μM each) before adding the solution to the reaction cell, with titrations individually performed using solutions of enantiomerically pure **4a** or **4b**. Heats of dilution were determined by titration of each ligand individually in Buffer A.

The experimental data were fitted to an *n*-equivalent binding site model using the nonlinear least-squares regression from the Origin software package (OriginLab Corp, Northampton, MA). Since the number of binding sites, *n*, converged to values between 0.9 and 1.1 in the initial regression analyses, a single-site binding model (1.0) was used for the final analyses. This yielded the following thermodynamic parameters: binding constant (K_d), binding enthalpy (ΔH) and the entropy change (ΔS), respectively.

Acknowledgements

This research was supported in part by the National Institutes of Health (GM66173), the United States Department of Agriculture (99-35103-8037), the National Science Foundation (MCB-0417291), the G. Thomas and Anita Hargrove Center for Plant Genomic Research, McIntire-Stennis, and the Murdock Charitable Trust. We thank D.J. Pouchnik for DNA sequencing and G. Munske for assistance with isothermal titration calorimetry; P.K. Lawrence also provided preliminary technical assistance in the mutagenesis experiments.

References

1 H. Adlercreutz, *J. Steroid Biochem. Mol. Biol.*, 2003, **83**, 113–118.
2 F. Boccardo, G. Lunardi, P. Guglielmini, M. Parodi, R. Murialdo, G. Schettini and A. Rubagotti, *Eur. J. Cancer*, 2004, **40**, 84–89.
3 P. Meresse, E. Dechaux, C. Monneret and E. Bertounesque, *Curr. Med. Chem.*, 2004, **11**, 2443–2466.
4 T. F. Imbert, *Biochimie*, 1998, **80**, 207–222.
5 R. M. Moraes, F. E. Dayan and C. Canel, *Stud. Nat. Prod. Chem.*, 2002, **26**, 149–182.
6 J. A. Gonzalez, A. Estevez-Braun, R. Estevez-Reyes, I. L. Bazzocchi, L. Moujir, I. A. Jimenez, A. G. Ravelo and A. G. Gonzalez, *Experientia*, 1995, **51**, 35–39.
7 C.-B. Bernard, J. T. Arnason, B. J. R. Philogène, J. Lam and T. Waddell, *Phytochemistry*, 1989, **28**, 1373–1377.
8 N. G. Lewis, L. B. Davin and S. Sarkanen, in *Comprehensive Natural Products Chemistry*, ed. Sir D. H. R. Barton, K. Nakanishi and O. Meth-Cohn, Elsevier, Oxford, 1999, vol. 3, p. 617–745.
9 N. G. Lewis, *Curr. Opin. Plant Biol.*, 1999, **2**, 153–162.
10 L. B. Davin and N. G. Lewis, *Curr. Opin. Biotechnol.*, 2005, **16**, 407–415.
11 A. Chu, A. Dinkova, L. B. Davin, D. L. Bedgar and N. G. Lewis, *J. Biol. Chem.*, 1993, **268**, 27026–27033.
12 A. T. Dinkova-Kostova, D. R. Gang, L. B. Davin, D. L. Bedgar, A. Chu and N. G. Lewis, *J. Biol. Chem.*, 1996, **271**, 29473–29482.
13 L. B. Davin, H.-B. Wang, A. L. Crowell, D. L. Bedgar, D. M. Martin, S. Sarkanen and N. G. Lewis, *Science*, 1997, **275**, 362–366.
14 M. Fujita, D. R. Gang, L. B. Davin and N. G. Lewis, *J. Biol. Chem.*, 1999, **274**, 618–627.
15 D. R. Gang, M. A. Costa, M. Fujita, A. T. Dinkova-Kostova, H.-B. Wang, V. Burlat, W. Martin, S. Sarkanen, L. B. Davin and N. G. Lewis, *Chem. Biol.*, 1999, **6**, 143–151.
16 N. G. Lewis and L. B. Davin, in *Comprehensive Natural Products Chemistry*, ed. Sir D. H. R. Barton, K. Nakanishi and O. Meth-Cohn, Elsevier, Oxford, 1999, vol. 1, p. 639-712.
17 Z.-Q. Xia, M. A. Costa, J. Proctor, L. B. Davin and N. G. Lewis, *Phytochemistry*, 2000, **55**, 537–549.
18 Z.-Q. Xia, M. A. Costa, H. C. Pélissier, L. B. Davin and N. G. Lewis, *J. Biol. Chem.*, 2001, **276**, 12614–12623.
19 S. C. Halls and N. G. Lewis, *Biochemistry*, 2002, **41**, 9455–9461.
20 T. Min, H. Kasahara, D. L. Bedgar, B. Youn, P. K. Lawrence, D. R. Gang, S. C. Halls, H. Park, J. L. Hilsenbeck, L. B. Davin, N. G. Lewis and C. Kang, *J. Biol. Chem.*, 2003, **278**, 50714–50723.
21 M.-H. Cho, S. G.A. Moinuddin, G. L. Helms, S. Hishiyama, D. Eichinger, L. B. Davin and N. G. Lewis, *Proc. Natl. Acad. Sci. U. S. A.*, 2003, **100**, 10641–10646.
22 L. B. Davin and N. G. Lewis, *Phytochem. Rev.*, 2003, **2**, 257–288.
23 S. G. A. Moinuddin, S. Hishiyama, M.-H. Cho, L. B. Davin and N. G. Lewis, *Org. Biomol. Chem.*, 2003, **1**, 2307–2313.
24 S. C. Halls, L. B. Davin, D. M. Kramer and N. G. Lewis, *Biochemistry*, 2004, **43**, 2587–2595.
25 B. Youn, S. G. A. Moinuddin, L. B. Davin, N. G. Lewis and C. Kang, *J. Biol. Chem.*, 2005, **280**, 12917–12926.
26 L. B. Davin and N. G. Lewis, *Curr. Opin. Biotechnol.*, 2005, **16**, 398–406.
27 H. Adlercreutz, *Bailliere's Clin. Endocrinol. Metab.*, 1998, **12**, 605–623.
28 A. Stark and Z. Madar, *J. Pediatr. Endocrinol. Metab.*, 2002, **15**, 561–572.
29 S. P. Borriello, K. D. R. Setchell, M. Axelson and A. M. Lawson, *J. Appl. Bacteriol.*, 1985, **58**, 37–43.
30 J. A. F. Gardner, G. M. Barton and H. MacLean, *Can. J. Chem.*, 1959, **37**, 1703–1709.
31 J. A. F. Gardner, B. F. MacDonald and H. MacLean, *Can. J. Chem.*, 1960, **38**, 2387–2394.
32 J. A. F. Gardner, E. P. Swan, S. A. Sutherland and H. MacLean, *Can. J. Chem.*, 1966, **44**, 52–58.
33 W. L. Duax, J. F. Griffin and D. Ghosh, *Curr. Opin. Struct. Biol.*, 1996, **6**, 813–823.
34 R. E. Viola, P. F. Cook and W. W. Cleland, *Anal. Biochem.*, 1979, **96**, 334–340.
35 N. J. Oppenheimer, L. J. Arnold and N. O. Kaplan, *Proc. Natl. Acad. Sci., U. S. A*, 1971, **68**, 3200–3205.
36 L. J. Arnold, Jr., K.-s. You, W. S. Allison and N. O. Kaplan, *Biochemistry*, 1976, **15**, 4844–4849.
37 K. Velonia, I. Tsigos, V. Bouriotis and I. Smonou, *Bioorg. Med. Chem. Lett.*, 1999, **9**, 65–68.
38 S. B. Mostad and A. Glasfeld, *J. Chem. Educ.*, 1993, **70**, 504–506.
39 P. E. Hansen, *Prog. Nucl. Magn. Reson. Spectrosc.*, 1988, **20**, 207–255.
40 N. J. Oppenheimer, *J. Biol. Chem.*, 1986, **261**, 12209–12212.
41 T. Wiseman, S. Williston, J. F. Brandts and L. N. Lin, *Anal. Biochem.*, 1989, **179**, 131–137.
42 I. Jelesarov and H. R. Bosshard, *J. Mol. Recognit.*, 1999, **12**, 3–18.
43 J. E. Ladbury, *BioTechniques*, 2004, **37**, 885–887.
44 U. Oppermann, C. Filling, M. Hult, N. Shafqat, X. Wu, M. Lindh, J. Shafqat, E. Nordling, Y. Kallberg, B. Persson and H. Jörnvall, *Chem.-Biol. Interact.*, 2003, **143–144**, 247–253.
45 T. Umezawa, L. B. Davin and N. G. Lewis, *J. Biol. Chem.*, 1991, **266**, 10210–10217.
46 D. S. Wishart, C. G. Bigam, J. Yao, F. Abildgaard, H. J. Dyson, E. Oldfield, J. L. Markley and B. D. Sykes, *J. Biomol. NMR*, 1995, **6**, 135–140.
47 J. C. Cobas and F. J. Sardina, *Concepts Magn. Reson., Part A*, 2003, **19A**, 80–96.
48 L. B. Davin, D. L. Bedgar, T. Katayama and N. G. Lewis, *Phytochemistry*, 1992, **31**, 3869–3874.
49 T. Katayama, L. B. Davin, A. Chu and N. G. Lewis, *Phytochemistry*, 1993, **33**, 581–591.
50 J. A. Anderson and B.-K. Lin, *Phytochemistry*, 1993, **32**, 811–812.
51 M. M. Bradford, *Anal. Biochem.*, 1976, **72**, 248–254.

